Characterizing the Chemical Behavior of Uranium Compounds for Nuclear Forensics

Marie C. Kirkegaard, Andrew Miskowiec, Michael W. Ambrogio, John Langford, Ashley E. Shields, Jennifer L. Niedziela, Roger Kapsimalis, Brian B. Anderson

Nuclear Security and Isotope Technology Division

Oak Ridge National Laboratory

Abstract

Better characterization of uranium compounds related to the nuclear fuel cycle is a key goal of the nuclear forensics community. Understanding the chemical behavior of these compounds in various environmental conditions and the effect on observable properties is crucial to the identification of unknown materials. Uranyl fluoride, the hydrolysis product of uranium hexafluoride, is a material of particular interest. Previous studies have suggested that uranyl fluoride may degrade upon exposure to high humidity, but the chemical pathway of degradation was previously not well understood. Our work demonstrates that uranyl fluoride undergoes a chemical reaction with water vapor to form uranyl hydroxide and peroxide species. This understanding will help guide forensic analysis in the future.

Introduction

Despite their prevalence in the nuclear fuel cycle, the chemistry of many uranium compounds is not well understood. In general, uranium systems have been studied with a focus on the production of bulk materials for the nuclear power industry. These research efforts have produced knowledge about basic physical properties, chemical form, and reactivity with respect to specific production or use cases. However, the body of open research and historical knowledge related to nuclear materials is not sufficient to understand uranium chemistry related to unknown or emerging processes. In addition, much of the research on uranium systems involves liquid or aqueous systems related to separations, environmental management, or interaction with biological systems. Although solid state systems have been studied for nuclear fuel development and nuclear materials management, detailed structural information is typically not available for fuel cycle by-products and mixed systems. Much of the structural information about solid uranium compounds arises from the study of uranium-containing minerals and is generally insufficient to identify new or unexplored man-made forms. The rigorous study of solid phase uranium compounds to develop a more comprehensive understanding of crystal structure, amorphous forms, and reactivity is necessary to advance the development of advanced fuels, nuclear materials management, environmental remediation and waste management, and nuclear forensics.

Advances in analytical tools and computational methods provide new approaches in the study of poorly characterized solid uranium materials. Anecdotal claims combined with conflicting research findings from “known” systems, indicating that these systems may not be correctly characterized, motivate the study of these materials using state-of-the-art tools, including neutron scattering methods, advanced spectroscopic methods, and structural elucidation tools applied to dynamic environments. The Nuclear Security Advanced Technologies Group at Oak Ridge National Laboratory focuses on the rigorous study of nuclear fuel cycle–relevant uranium materials to understand the structure and chemistry of systems such as uranium oxyfluorides, mixed uranium fluorides, and crystalline and amorphous uranium oxides with the goal of applying advanced microanalytical tools to characterizing materials in bulk and particulate forms

and relating measurements from different scales. This approach involves the preparation of uranium solid materials and full characterization utilizing electron microscopy with elemental analysis, X-ray diffraction, inelastic neutron scattering, and powder neutron diffraction. When combined with theoretical methods that relate known structural information with predicted vibrational spectral information, these techniques provide a rigorous approach for relating observables from previously unknown structures to known structures under study. In addition, many of the techniques used for structural/chemical characterization are applied under both static and dynamic environmental conditions (water vapor pressure and temperature) to understand solid phase transitions between known forms and new, unexplored structures. We have used such an approach to study the chemistry of uranyl fluoride (UO_2F_2), an intermediate in the nuclear fuel cycle of interest to the nuclear forensics community.

Uranyl Fluoride

Uranyl fluoride (UO_2F_2) is the hydrolysis product of uranium hexafluoride (UF_6) via the following reaction: $UF_6 + 2H_2O \rightarrow UO_2F_2 + 4HF$. Uranyl fluoride is of significant interest to the nuclear forensics community because it is produced when traces of UF_6 interact with moisture in the environment. Characterizing the chemical behavior of uranyl fluoride in various environmental conditions is crucial for correlating laboratory measurements to the material history.

Phase Transition between Anhydrous and Hydrated Uranyl Fluoride

Uranyl fluoride exists in the form of an anhydrous crystal and at least one crystal hydrate. Anhydrous uranyl fluoride has a hexagonal layered structure, as shown in Figure 1.[1,2] It is hygroscopic and absorbs some amount of water between each layer without a significant change in the crystal structure.[3–5] At moderate humidity, the anhydrous crystal converts to a stable hydrate form, originally identified as having between 1.5 and 2 waters per uranium.[3,4,6]

In 2001, Mikhailov et al. solved the structure of a uranyl fluoride hydrate of the form $[(UO_2F_2)(H_2O)]_7 \cdot 4H_2O$, with 1.57 waters per uranium. This hydrate, shown in Figure 2, has pentagonal coordination of the uranyl ion with four fluorine equatorial ligands and one water ligand. This hydrate was not produced from the hydration of anhydrous uranyl fluoride but rather by the reaction of uranyl acetate dihydrate in n-perfluoropropoxy-1-perfluoropropionic acid.[7] However, the stability of this hydrate and measured water content suggested that it could be the hydrate observed to form at ambient conditions in previous studies.

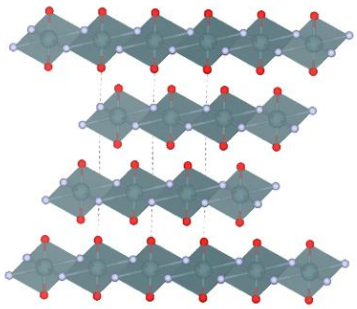

Figure 1. The structure of anhydrous uranyl fluoride, UO_2F_2.

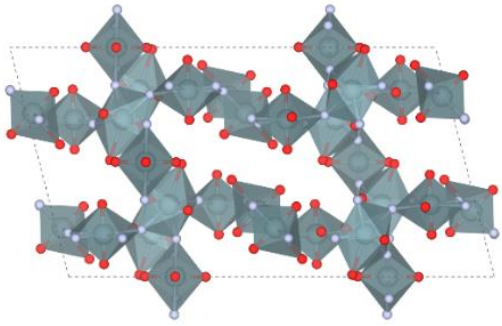

Figure 2. The structure of hydrated uranyl fluoride, $[(UO_2F_2)(H_2O)]_7*4H_2O$. Hydrogens and hydrogen-bonded water molecules have been omitted for clarity.

We demonstrated via neutron diffraction that the Mikhailov structure can be produced by hydrating anhydrous uranyl fluoride with gas phase water at ambient temperatures (40% relative humidity [RH]) and then desiccating the hydrated material.[8] A liquid-like intermediate with little long-range order, which we have called "L," was also observed in this transition (Figure 3). We have proposed that this liquid-like state is a necessary intermediate because a solid-state transition between the anhydrous and hydrated structures is not symmetry-allowed.[8] Pair distribution function measurements showed that the uranyl ion is pentagonally coordinated in L, as in the hydrated structure. Thus, a change in coordination number from six to five occurs in the transition between the anhydrous crystal and liquid-like intermediate.[8]

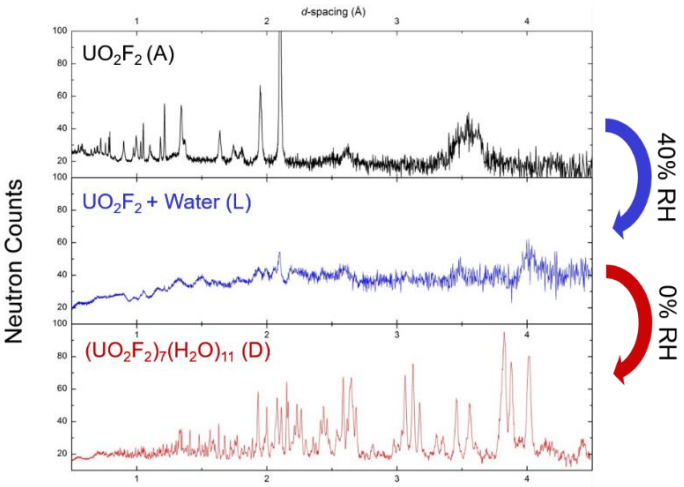

Figure 3. Neutron diffraction patterns of (A) anhydrous uranyl fluoride initially, (L) after exposure to 40% RH, and (D) after desiccation. The diffraction pattern after desiccation matches of $[(UO_2F_2)(H_2O)]_7{\cdot}4H_2O$).

This system was also studied via in-situ quasi-elastic neutron scattering. Anhydrous and hydrated uranyl fluoride can be differentiated via quasi-elastic neutron scattering because the water dynamics differ in the two structures. In this experiment, uranyl fluoride was exposed to controlled RH for 86 hours. The observed increase in quasi-elastic intensity demonstrated that the amount of water that enters the crystal structure is proportional to the water vapor pressure. This confirmed that water vapor pressure is the driving thermodynamic force for the conversion of anhydrous uranyl fluoride to hydrated uranyl fluoride.[9]

In-situ Raman spectroscopy proved similarly useful for studying this transition. Since the Raman-active uranyl symmetric stretching mode is highly sensitive to the environment of the uranyl ion, anhydrous and hydrated uranyl fluoride can be easily distinguished using Raman spectroscopy, with Raman-active uranyl stretching frequencies of 915 and 868 cm^{-1}, respectively

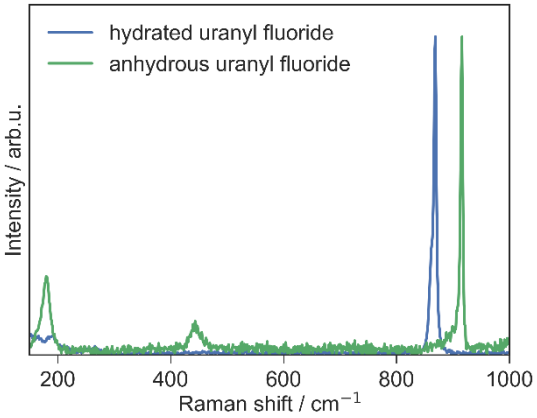

Figure 4. Raman spectra of hydrated and anhydrous uranyl fluoride.

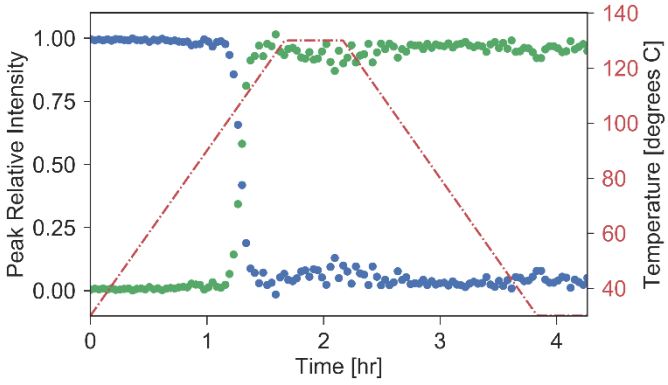

Figure 5. Relative intensity of peaks corresponding to hydrated uranyl fluoride (868 cm^{-1}, blue) and anhydrous uranyl fluoride (915 cm^{-1}, green) as the temperature was ramped from 30°C to 130°C and back to 30°C.

(Figure 4).[10-13] In-situ Raman spectroscopy studies with temperature control confirmed that the dehydration transition occurs around 125°C in air (Figure 5), in agreement with thermogravimetric analysis.[8,13] Although this dehydration was found to be irreversible at ambient humidity (~30–40%RH) in the short-term, rehydration occurs readily at 50% RH (Figure 6). This suggests that the desiccation step taken in the neutron diffraction experiment is not a requisite to producing hydrated uranyl fluoride, although it is hard to assess crystallinity from Raman spectra.

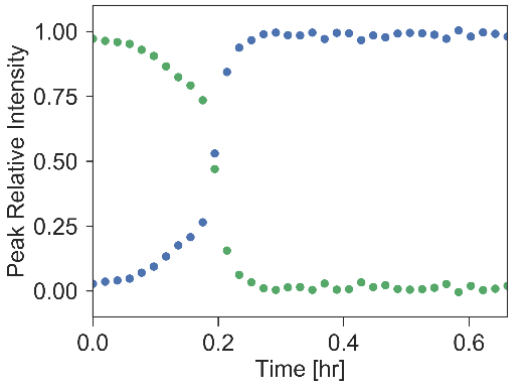

Figure 6. Relative intensity of peaks corresponding to hydrated uranyl fluoride (868 cm^{-1}, blue) and anhydrous uranyl fluoride (915 cm^{-1}, green) as anhydrous uranyl fluoride was exposed to 50% RH at 30°C.

In summary, we used a variety of complementary in-situ techniques to clarify the relationship between anhydrous and hydrated uranyl fluoride, showing conclusively that a uranyl fluoride hydrate of the form $[(UO_2F_2)(H_2O)]_7 \cdot 4H_2O$ can be produced by exposing anhydrous uranyl fluoride to a humid environment and converted back to anhydrous uranyl fluoride by heating to about 125°C.

Chemical Transformation of Hydrated Uranyl Fluoride

Although the Mikhailov hydrate ($[(UO_2F_2)(H_2O)]_7 \cdot 4H_2O$) is the only uranyl fluoride hydrate structure that has been solved, previous studies suggest that additional hydrates may exist at higher water vapor pressures. For example, Marshall et al. suggested the existence of three different hydrates with the same approximate composition, $UO_2F_2 \cdot 2H_2O$.[14] Brooks et al. tentatively identified the formation of a trihydrate after equilibrating material at 100% RH for 144 hours.[6] Gromov and colleagues identified four distinct hydrates with X-ray and equilibrium vapor pressure measurements that could be formed by equilibrating uranyl fluoride powder with water vapor at varying temperatures over 2–8 weeks.[15,16] On the other hand, Lychev et al. did not observe the formation of any additional species at elevated water vapor pressure.[4] The current literature thus leaves uncertainty about how many uranyl fluoride hydrates may exist. None of the above studies provide conclusive identification of the crystal structures, meaning that it is feasible that some of the species observed may not have actually been uranyl fluoride hydrates, but rather other uranyl species produced through a chemical reaction with water vapor.

More recently, Kips et al. studied how exposure to water vapor alters the Raman signature of hydrated uranyl fluoride. Upon long-term exposure to a humid environment, an additional red-shifted uranyl stretching mode around 845 cm^{-1} was observed in the Raman spectra and attributed to the absorption of water in the uranyl fluoride hydrate structure.[17,18] Kips et al. also raised the possibility that uranyl fluoride undergoes a loss of fluorine upon exposure to elevated water pressure. Using scanning electron microscopy with energy dispersive X-ray spectroscopy (SEM-EDS) and ion-microprobe secondary ion mass spectrometry (IM-SIMS), they measured a reduction in the F/U ratio of uranyl fluoride particles after aging for 28 months.[11] This supports the possibility that a chemical reaction with water vapor produces additional uranyl species. This measured loss of fluorine was not correlated with observed changes in the Raman spectrum, leaving uncertainty about whether the additional peaks in the Raman spectra after hydration could be attributed to species other than uranyl fluoride hydrates.

We assessed the stability of the Mikhailov hydrate by exposing particles of uranyl fluoride (made from depleted source material) to various temperatures and humidities. Particles were deposited on adhesive carbon tabs and enclosed in plastic containers that contained saturated salt solutions. The containers were split between two incubators, one at 21°C and one at 35°C. Over the course of a few months, the particles were analyzed via Raman spectroscopy through a glass window in the lid of the plastic containers.

All of the initial Raman spectra were characteristic of the Mikhailov hydrate, with a dominant uranyl stretching peak at 868 cm^{-1}. Changes in the Raman spectra were observed over time, however, especially for the samples at higher temperature and humidity. These changes were most notable in the uranyl stretching region (700–950 cm^{-1}), where two additional peaks grew in: one at 845 cm^{-1} matching previous findings by Kips et al. and one at 820 cm^{-1} (Figure 7). Figure 8 shows the relative intensities of these peaks over time for each sample. At 59% and 75% RH, a significant decrease in the intensity of the peak at 868 cm^{-1} suggests the degradation of the Mikhailov hydrate. As the peak at 868 cm^{-1} decreases, the peak at 845 cm^{-1} increases in relative intensity, along with the peak at 820 cm^{-1} to a lesser extent. This transformation occurs more rapidly at elevated temperature (35°C). Interestingly, at 35°C and 75% RH, the peak at 845 cm^{-1} decreases in relative intensity after rapidly growing in, whereas the peak at 868 cm^{-1} appears to grow in relative intensity after nearly disappearing.

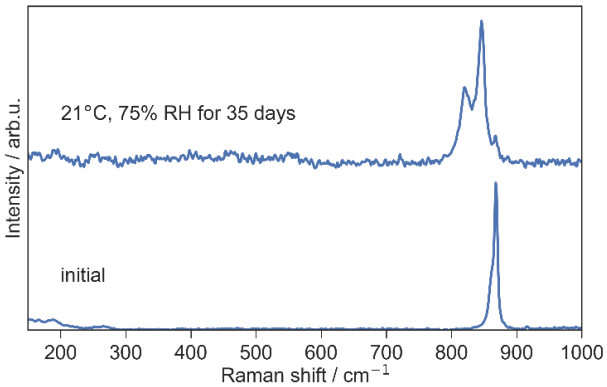

Figure 7. Raman spectrum of a uranyl fluoride particle initially (below) and after exposure to 75% RH for 35 days (above).

Figure 8 shows that some changes occurred in the spectra of samples stored at lower humidities as well. Since the initial material was not desiccated before use, it is likely that physiosorbed water was present on the surface of the particles at the beginning of the experiment. This could explain

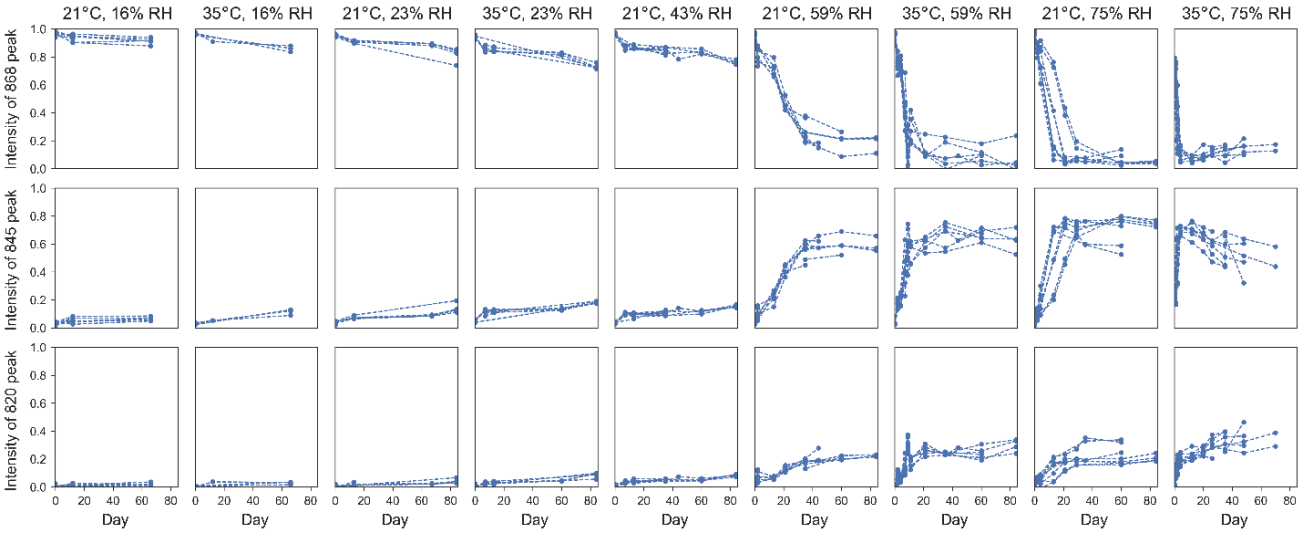

Figure 8. Relative intensities of peaks at 868 cm^{-1}, 845 cm^{-1}, and 820 cm^{-1} for each sample. Multiple points on the same day correspond to different particles. Points connected by dashed lines correspond to the same particle. Variation in the transformation rate of different particles on the same sample is likely due to variation in particle size.

why the Mikhailov hydrate does not appear to be stable even at low humidity. The growth of the peak at 845 cm^{-1} in these samples was much less significant than the fairly rapid transformation at elevated water vapor pressure.

This transformation at elevated water vapor pressure was further assessed with an extended particle hydration study.[19] Particles of uranyl fluoride hydrate were again deposited on multiple adhesive carbon tabs and exposed to the headspace of a NaCl saturated salt solution to provide 75% RH. Samples were left at room temperature (20–23°C) throughout the course of the 238-day experiment, and changes in the particles were monitored throughout this time via micro-Raman spectroscopy. The same particles were observed throughout the study.

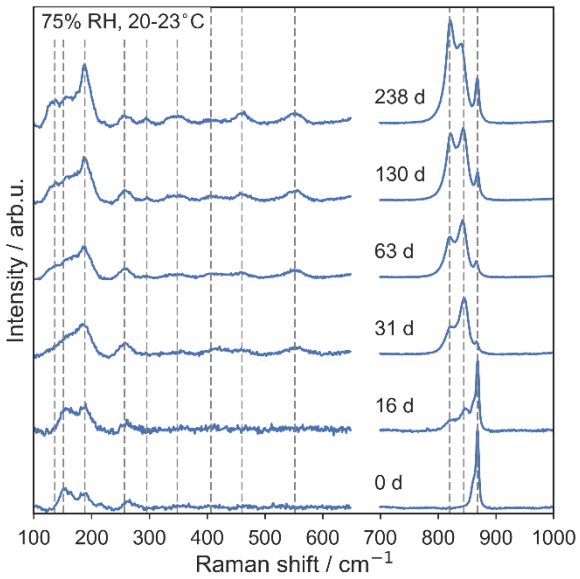

Figure 9. Raman spectra of a uranyl fluoride particle exposed to 75% RH for varying amounts of time. Vertical lines show the positions of peaks at 136, 151, 188, 236, 257, 295, 348, 406, 460, 552, 820, 845, and 868 cm^{-1}.

Once again, additional Raman peaks were observed to grow in the uranyl stretching region at 845 and 820 cm^{-1}, whereas the 868 cm^{-1} peak characteristic of the Mikhailov hydrate decreased in intensity (Figure 9). Over the first 31 days, significant color changes were observed for these particles as well, as shown in Figure 10. After this time, the color appeared relatively consistent, although the Raman spectra continued to change through the end of the experiment. As observed in the previous study, the peak at 868 cm^{-1} began to grow in intensity with further hydration after largely disappearing in the first 31 days of hydration. After 190 days of equilibrating at 75% RH, the NaCl-saturated salt solution in one of the samples was replaced with deionized water to further increase the water vapor pressure. This led to the rapid growth of peaks at 820 and 866 cm^{-1} and the complete disappearance of the peak at 845 cm^{-1} (Figure 11). After 48 days at 100% RH, no further changes were observed in the Raman spectrum.

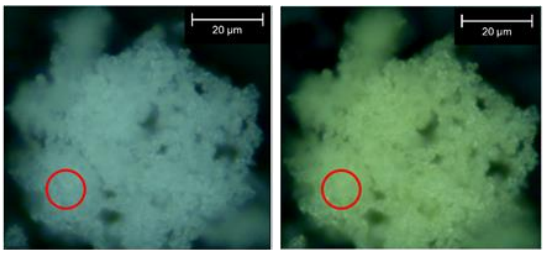

Figure 10. Microscope images of a uranyl fluoride particle initially (left) and after hydrating at 75% RH for 31 days (right). The red circles identify where Raman spectra were collected at each date.

At the conclusion of the experiment, energy dispersive X-ray spectroscopy (EDS) was used to perform a qualitative elemental analysis of the two hydrated samples and a sample of fresh uranyl fluoride particles. In the EDS spectra of a fresh uranyl fluoride particle (Figure 11, bottom left), the uranium M-peaks (3.17 and 3.34 keV), fluorine K-peak (0.67 keV), and oxygen K-peak (0.53 keV) are all clearly visible, and no obvious contaminants were observed. Peaks associated with carbon appear in all samples because of the substrate, and peaks associated with nitrogen were presumed to be due to the release of entrained N_2 from the interstices of the particles under vacuum. In the EDS spectra of both hydrated samples (Figure 11, bottom middle and right), the fluorine EDS peak was no longer observed, while the uranium and oxygen peaks remained.

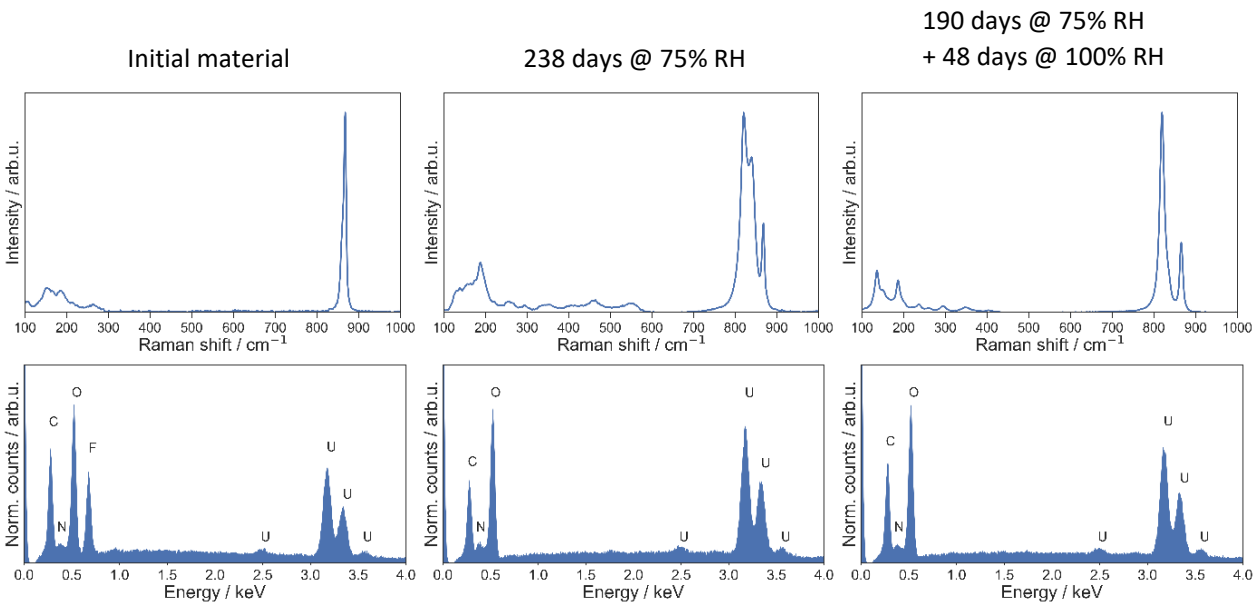

Figure 11. Raman (above) and EDS spectra (below) of a characteristic uranyl fluoride particle initially (left), characteristic uranyl fluoride particle exposed to 75% RH for 238 days (center), and characteristic uranyl fluoride particle exposed to 75% RH for 190 days and then 100% RH for an additional 48 days (right).

It is apparent from Figure 11 that uranyl fluoride undergoes a loss of fluorine at elevated water vapor pressure. Although the EDS spectra were not necessarily collected on the same particles studied via Raman spectroscopy, EDS spectra were consistent across multiple particles on the same sample. Thus, it is clear that neither hydrated sample contained an appreciable amount of fluorine, and that none of the Raman peaks in the hydrated samples (Figure 11, top-middle and right) can be attributed to uranyl fluoride. Consequently, the peak near 868 cm^{-1} in these spectra cannot indicate the presence of $[(UO_2F_2)(H_2O)]_7 \bullet 4H_2O$ and must instead be related to a mode in a different species with a coincidentally similar frequency.

This species can be identified by comparing the fully hydrated Raman spectrum (Figure 11, top-right) with that of the uranyl peroxide species studtite, $[(UO_2)(O_2)(H_2O)_2] \bullet (H_2O)_2$.[20] Studtite has been well-characterized via Raman spectroscopy and is known to exhibit a peak at 820 cm^{-1} (assigned to the symmetric uranyl stretch) and a peak at 868 cm^{-1} (assigned to the peroxide stretch).[12,21–26] Figure 12 shows a comparison of the spectrum of a fully hydrated particle and that of synthetic studtite (structure verified via X-ray powder diffraction). Excellent agreement is noted not only for the 700–1,000 cm^{-1} region but also for the lower peaks as well, clearly identifying the

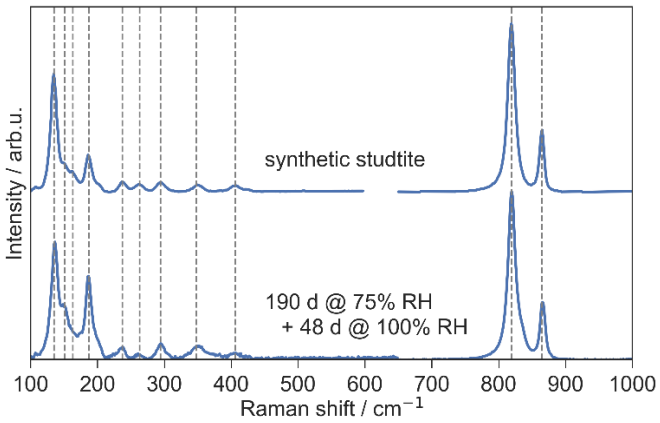

Figure 12. Raman spectrum of a uranyl fluoride particle hydrated at 75% RH for 190 days + 100% RH for 48 days (below) compared to the Raman spectrum of synthetic studtite (above). Vertical lines show the positions of peaks at 135, 151, 163, 187, 237, 263, 294, 348, 406, 819, and 864 cm^{-1}.

particle as a uranyl peroxide species. The formation of a uranyl peroxide species is further supported by the fact that following vacuum exposure during SEM-EDS analysis, the Raman spectra of the fully hydrated particles matched those reported for metastudtite, the dehydration product of studtite, with a uranyl stretching mode at 830 cm^{-1}.[22,24]

Returning to Figure 11, it is now clear that the particles kept at 75% RH throughout the duration of the experiment underwent an incomplete transformation to the same uranyl peroxide species observed at 100% RH. After 238 days of hydration at 75% RH, the particles were composed of a mix of two hydration products: uranyl peroxide and a second intermediate species with dominant peaks at 845, 552, and 460 cm^{-1}. This species cannot be another uranyl fluoride hydrate because the corresponding EDS spectrum shows a lack of measurable fluorine. Instead, we identify this species as a uranyl hydroxide hydrate based on a comparison to the Raman spectra of uranyl hydroxide species like metaschoepite, which typically have a symmetric uranyl stretching frequency in the 830–855 cm^{-1} range, as well as peaks near 550 and 450 cm^{-1}.[12,21,23,25,27–30] We propose that at elevated water vapor pressure, water molecules interact with the bridging fluorine ligands in $[(UO_2F_2)(H_2O)]_7 \bullet 4H_2O$, forming hydroxyl bridges and releasing HF gas from the crystal matrix.[19] However, the reported Raman spectra for uranyl hydroxides are not very consistent,[12,21,23,25,27–30] making identification of the species difficult from Raman data alone. Inconsistency in the literature is due in part to the challenge of making pure uranyl hydroxide species, which is compounded by the fact that multiple uranyl hydroxide hydrates interconvert at ambient conditions.[31,32] Ongoing computational work may help clarify the vibrational spectra of "pure" uranyl hydroxide species that are difficult to study experimentally.

To better understand the structure of the uranyl hydroxide hydration product, the hydration of uranyl fluoride was also studied via X-ray diffraction. Loose uranyl fluoride powder was placed on a silicon X-ray plate along with LaB_6 powder to serve as a reference material. After an initial scan, the X-ray plate was placed in a 35°C incubator and exposed to a NaCl-saturated salt solution to hydrate at 75% RH. The sample was occasionally removed to collect both Raman and X-ray data. After 26 days, Raman spectra showed clear peaks at 820 and 845 cm^{-1}. The corresponding X-ray pattern shows the growth of peaks that are reasonably consistent with the uranyl hydroxide hydrate schoepite (Figure 13). Despite the presence of peaks attributed to uranyl peroxide in the Raman spectrum, the X-ray pattern of the hydrated material does not show evidence of the presence of a uranyl peroxide species. It is possible that the component is too small of a fraction to observe via X-ray diffraction, or that it is amorphous.

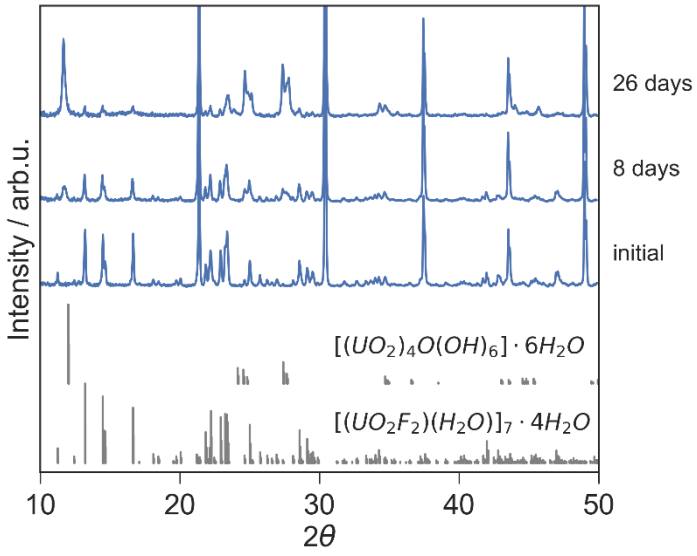

Figure 13. X-ray patterns of uranyl fluoride powder exposed to 35°C and 75% RH for varying amounts of time. Sharp peaks at 2Θ = 21.36, 30.38, 37.44, 43.51, and 48.96 correspond to the LaB_6 reference.

The structure of the species still cannot be conclusively identified, however, because crystal hydrates that differ primarily in water organization cannot

be well-distinguished via powder X-ray diffraction. For example, the uranyl hydroxide hydrates schoepite and metaschoepite have very similar powder X-ray diffraction patterns.[32,33] In this case, understanding the water structure of the observed species is especially important because the water vapor pressure is a driving factor in the transition from uranyl fluoride to the uranyl hydroxide and uranyl peroxide species. Consequently, clarifying the water structure could shed light on the formation mechanism of the peroxide species, which remains unclear. Neutron diffraction improves the identification of the water structure in crystal hydrates because neutrons are much more sensitive to light elements like hydrogen than X-rays. Neutron diffraction studies are therefore planned as part of this ongoing study. Studying several uranyl hydroxide species using both neutron diffraction and vibrational spectroscopy techniques will also allow for the correlation of data sets, which will aid in future identification of materials when only one technique is available or appropriate.

In summary, because of uncertainties in the literature, we sought to clarify the chemical behavior of uranyl fluoride at elevated water vapor pressure. We have demonstrated that at elevated water vapor pressure, uranyl fluoride is not stable but rather undergoes a transformation to uranyl hydroxide and ultimately to uranyl peroxide. The observed uranyl hydroxide intermediate appears similar in structure to the uranyl hydroxide hydrates schoepite and metaschoepite. The mechanism by which peroxo groups form from this hydroxide intermediate remains unclear. The same hydration reaction has been observed in the dark, demonstrating that the reaction is not photochemical.[19] Additionally, although uranyl peroxide species have been observed to form in environments where significant radiation leads to the in-situ production of hydrogen peroxide via water radiolysis, the depleted source material used in these studies does not have the alpha activity to promote such a reaction. It thus seems likely that a novel formation mechanism for uranyl peroxide exists, driven by water vapor pressure. Additional work is necessary to understand the underlying chemistry of this reaction.

References

1. Zachariasen, F. W. H. Crystal chemical studies of the 5*f*-series of elements. III. A study of the disorder in the crystal structure of anhydrous uranyl fluoride. *Acta Crystallogr.* **1,** 277–281 (1948).
2. Atoji, M. & McDermott, M. J. The crystal structure of anhydrous UO_2F_2. *Acta Crystallogr. Sect. B Struct. Crystallogr. Cryst. Chem.* **26,** 1540–1544 (1970).
3. Morato, F., Fulconis, J. M., Rouquerol, F. & Fourcade, R. Study of the dehydration process of uranyl difluoride hydrates stable under usual conditions of temperature, pressure, and atmospheric moisture. *J. Fluor. Chem.* **91,** 69–73 (1998).
4. Lychev, A. A., Mikhalev, V. A. & Sublobov, D. N. Crystalline hydrates of uranyl fluoride at 20°C. *Radiokhimiya* **32,** 7–12 (1990).
5. Miskowiec, A. *et al.* Structural phase transitions and water dynamics in uranyl fluoride hydrates. *J. Phys. Chem. A* **119,** (2015).
6. Brooks, L. H., Garner, E. V. & Whitehead, E. Chemical and X-ray crystallographic studies on uranyl fluoride. Report no. IGR-TN/CA-277, United Kingdom Atomic Energy Authority (1956).
7. Yu. N. Mikhailov, Yu. E. Gorbunova, I. P. Stolyarov & I. I. Moiseev. A new modification of monoaquadifluorouranyl hydrate. *Dokl. Chem.* **380,** 293–297 (2001).
8. Miskowiec, A. *et al.* Structural phase transitions and water dynamics in uranyl fluoride hydrates. *J. Phys. Chem. A* **119,** 11900–11910 (2015).
9. Miskowiec, A. *et al.* Quasielastic neutron scattering with in situ humidity control: Water dynamics in uranyl fluoride. *J. Appl. Phys.* **119,** (2016).
10. Armstrong, D. P., Jarabek, R. J. & Fletcher, W. H. Micro-Raman spectroscopy of selected solid $U_xO_yF_z$ compounds. *Appl. Spectrosc.* **43,** 461–468 (1989).
11. Kips, R. *et al.* Determination of fluorine in uranium oxyfluoride particles as an indicator of particle age. *Spectrochim. Acta: Part B At. Spectrosc.* **64,** 199–207 (2009).

12. Pointurier, F. & Marie, O. Identification of the chemical forms of uranium compounds in micrometer-size particles by means of micro-Raman spectrometry and scanning electron microscope. *Spectrochim. Acta: Part B At. Spectrosc.* **65,** 797–804 (2010).
13. Kirkegaard, M. C., Langford, J., Steill, J., Anderson, B. B. & Miskowiec, A. Vibrational properties of anhydrous and partially hydrated uranyl fluoride. *J. Chem. Phys.* **146** (2017).
14. Marshall, W. L., Gill, J. S. & Secoy, C. H. Phase equilibria of uranium trioxide and aqueous hydrofluoric acid in stoichiometric concentrations. *J. Am. Chem. Soc.* **76,** 4279–4281 (1954).
15. Tsvetkov, A. A., Seleznev, V. P., Sudarikov, B. N. & Gromov, B. V. Equilibrium diagram of the uranyl fluoride-water system. *Russ. J. Inorg. Chem.* **17,** 1048–1050 (1972).
16. Seleznev, V. P., Tsvetkov, A. A., Sudarikov, B. N. & Gromov, B. V. Uranyl fluoride hydrates. *Russ. J. Inorg. Chem.* **17,** 1356–1357 (1972).
17. Kips, R., Crowhurst, J., Kristo, M. J., Stefaniak, E. & Hutcheon, D. Micro-Raman spectroscopy of uranium oxyfluoride particulate material for nuclear safeguards. Report no. LLNL-PROC-433314, Lawrence Livermore National Laboratory, Livermore, CA (2010).
18. Stefaniak, E. A. *et al.* New insight into UO_2F_2 particulate structure by micro-Raman spectroscopy. *J. Mol. Struct.* **1040,** 206–212 (2013).
19. Kirkegaard, M. C., Miskowiec, A., Ambrogio, M. W. & Anderson, B. B. Evidence of a nonphotochemical mechanism for the solid-state formation of uranyl peroxide. *Inorg. Chem.* **57**, 10, 5711-5715 (2018).
20. Burns, P. C. & Hughes, K.-A. Studtite, $[(UO_2)(O_2)(H_2O)_2](H_2O)_2$: The first structure of a peroxide mineral. *Am. Mineral.* **88,** 1165–1168 (2003).
21. Amme, M. *et al.* Raman microspectrometric identification of corrosion products formed on UO_2 nuclear fuel during leaching experiments. *J. Nucl. Mater.* **306,** 202–212 (2002).
22. Bastians, S., Crump, G., Griffith, W. P. & Withnall, R. Raspite and studtite: Raman spectra of two unique minerals. *J. Raman Spectrosc.* **35,** 726–731 (2004).
23. Canizares, A. *et al.* In situ Raman monitoring of materials under irradiation: Study of uranium dioxide alteration by water radiolysis. *J. Raman Spectrosc.* **43,** 1492–1497 (2012).
24. Labs, S. Secondary uranium phases of spent nuclear fuel: Coffinite, $USiO_4$, and studtite, $UO_4.4H_2O$—Synthesis, characterization, and investigations regarding phase stability. *Schriften des Forschungszentrums Jülich* **267,** (2015).
25. Berlizov, A., Ho Mer Lin, D., Nicholl, A., Fanghänel, T. & Mayer, K. Assessing hand-held Raman spectrometer FirstDefender RM for nuclear safeguards applications. *J. Radioanal. Nucl. Chem.* **307,** 285–295 (2016).
26. Colmenero, F., Bonales, L. J., Cobos, J. & Timón, V. Study of the thermal stability of studtite by in situ Raman spectroscopy and DFT calculations. *Spectrochim. Acta Part A Mol. Biomol. Spectrosc.* **174,** 245–253 (2017).
27. Frost, R. L., Cejka, J. & Weier, M. L. Raman spectroscopic study of the uranyl oxyhydroxide hydrates: Becquerelite, billietite, curite, schoepite and vandendriesscheite. *J. Raman Spectrosc.* **38,** 460–466 (2007).
28. Alam, T. M., Liao, Z., Nyman, M. & Yates, J. Insight into hydrogen bonding of uranyl hydroxide layers and capsules by use of ^{1}H magic-angle spinning NMR spectroscopy. *J. Phys. Chem. C* **120,** 10675–10685 (2016).
29. Ho Mer Lin, D., Manara, D., Lindqvist-Reis, P., Fanghanel, T. & Mayer, K. The use of different dispersive Raman spectrometers for the analysis of uranium compounds. *Vib. Spectrosc.* **73,** 102–110 (2014).
30. Ho Mer Lin, D. *et al.* Raman spectroscopy of uranium compounds and the use of multivariate analysis for visualization and classification. *Forensic Sci. Int.* **251,** 61–68 (2015).
31. Finch, R. J., Hawthorne, F. C., Miller, M. L. & Ewing, R. C. Distinguishing among schoepite, $[(UO_2)_8O_2(OH)_{12}](H_2O)_{12}$, and related minerals by X-ray powder diffraction. *Powder Diffr.* **12,** 230–238 (1997).
32. Finch, R. J., Hawthorne, F. C. & Ewing, R. C. Structural relations metaschoepite and "dehydrated schoepite." *Can. Mineral.* **36,** 831–845 (1998).
33. Weller, M. T., Light, M. E. & Gelbrich, T. Structure of uranium(VI) oxide dihydrate, $UO_3{\cdot}2H_2O$; synthetic meta-schoepite $(UO_2)_4O(OH)_6{\cdot}5H_2O$. *Acta Crystallogr. Sect. B Struct. Sci.* **56,** 577–583 (2000).